Journal of Applied Electrochemistry (2005) 35:421–427
DOI 10.1007/s10800-004-8349-z

Electrochemical reduction of nitrate ion on various cathodes – reaction kinetics on bronze cathode

C. POLATIDES and G. KYRIACOU*
Department of Chemical Engineering, Laboratory of Inorganic Chemistry, Aristotle University of Thessaloniki, Thessaloniki 541 24, Greece
*(*author for correspondence, e-mail: kyriakou@vergina.eng.auth.gr; fax: +30-231-996193)*

Received 19 July 2004; accepted 06 December 2004

Key words: electrochemical, kinetic analysis, nitrate, reduction, removal

Abstract

The electrochemical reduction of NO_3^- in 0.1 M K_2SO_4 and 0.05 M KNO_3 solution was studied on various electrodes in two different cell configurations, a divided and an undivided one. The products in all cases were NO_2^-, NH_3, N_2 and small amounts of NO_2 and NO. The more efficient cathodes as regards the conversion of NO_3^- to N_2 were Al and the alloy Sn85Cu15, where the selectivity for nitrogen formation was 43 and 35.3% at −1.8 and −2.0 V, respectively. The kinetic analysis of the experimental results was carried out by numerical solution of the resulted differential equations according to the scheme:

$$NO_3^- \xrightarrow{k_1} NO_2^- \xrightarrow{k_2} NH_3$$

$$NO_2^- \xrightarrow{k_3} N_2$$

The rate constants on Sn85Cu15 at −2.0 V for the above reactions were found to be $k_1 = 4.9 \times 10^{-4}$ s^{-1}, $k_2 = 1.76 \times 10^{-5}$ s^{-1} and $k_3 = 7.66 \times 10^{-3}$ l mol^{-1} s^{-1}. At more negative potential more NO_2^- ions reduced and converted either to N_2 or NH_3. The rate constant of reduction of nitrate was almost the same in the region between −1.7 and −2.0 V, because the reaction is limited by the diffusion. In order to oxidize a part of the undesirable byproducts NO_2^- and NH_3 at the anode of the cell to nitrate and nitrogen respectively, an undivided cell was used. Comparison between the two cell configurations indicated that, although in the undivided cell the % removal efficiency of nitrate was lower than that in the divided one, the selectivities of NO_2^- and NH_3 were 4.8 and 2.2 times lower, respectively.

1. Introduction

Nitrate is a worldwide groundwater contaminant mainly due to the use of nitrogen fertilizers, industrial wastes as well as animal wastes and septic systems [1]. High concentration of nitrate in potable water can cause several health problems such as the "blue baby syndrome" in infants, liver damage and cancer. The maximum contaminant level (MCL) in wastewaters and potable water is 45 mg l^{-1} in the United States, while in the European Union is 50 and 15 mg l^{-1} for infants [2, 3].

Various methods such as biological, physicochemical, chemical and electrochemical have been proposed for the removal of nitrate from potable water and wastewaters. Even though biological denitrification is the method of choice it has various disadvantages e.g. it is slow, difficult to control, produces organic residues and requires intensive maintenance and a constant supply of the organic substrate [4]. Furthermore, it can be used only at concentrations lower than 1000 mg l^{-1}, since higher ones can be poisonous to the bacteria. The physicochemical processes such as ion exchange [5], reverse osmosis [6] and electrodialysis [7] produce secondary brine wastes, because the nitrates are merely separated but not destroyed. The chemical methods produce toxic byproducts, such as nitrite and ammonia and require either large quantities of metals [8–11] or hydrogen as reducing agent, which is an unsafe and difficult to handle gas [12–14].

Electrocatalytic processes have been extensively studied in the last 30 years [15–21]. Three different ways of electrocatalytic reduction of nitrates are known [5]: (i) addition of electrocatalytically active ions such as VO_3^-,

MoO_4^{2-}, WO_4^{2-} or cobalt complexes [22] directly to the treated solution (ii) immobilization of the catalyst on the cathode surface, for example, carbon electrode modified with phthalocyanine complexes [23] and (iii) electrocatalytic reduction on solid electrodes [15–21]. Many solid electrodes have been tested including Pb [18, 19, 24], Ni [18, 19, 24, 25], Fe [19, 24], Cu[15, 23, 25, 26], Pt[16, 27, 28], Zn[29], Ru[30], Pd[26, 30, 31], C[21, 24, 25] and Ir[16, 30]. Among these, copper was shown to be the most efficient electrocatalyst [32] concerning the rate of the nitrate reduction.

The main problems in the electrocatalytic reduction of nitrates on solid electrodes are the low rate of reduction and the production of more toxic byproducts than nitrates, such as NO_2^-, NH_3 and NH_2OH. The electrochemical methods are ideal for the removal of nitrate from the concentrated secondary brine produced from the physicochemical methods and from water solutions containing poisonous compounds, such as nuclear wastes [19, 24], where the biological denitrification cannot be applied. This work deals with the electrochemical reduction of nitrates on different electrodes including lead, zinc, aluminum, copper and copper alloys in two different cell configurations, divided and undivided. The byproducts such as nitrite and ammonia can be partially oxidized on the anode of the undivided cell to nitrate and gaseous products respectively. The experiments were performed in a neutral solution, which resembles the natural waters. Moreover, this work includes kinetic analysis of the experimental results and the influence of potential on the product distribution.

2. Experimental details

2.1. *Cell, materials and electrodes*

A Teflon electrochemical cell having a total volume of 40 ml was used in all experiments. A Nafion 117 (H^+ form) cation exchange membrane divided the cell into two equal volume compartments. In the undivided cell the anodic compartment and the Nafion membrane were not used. The geometrical area of the cathode was 12.56 cm^2 and the anode was a platinized Pt foil (Alpha Metal) of equal area. The potential was controlled by a Wenking LB 81 H (Bank Elektronik) potentiostat and the reference was a saturated Ag/AgCl electrode. Ultra pure water (Sation 9000) was used for the preparation of the solutions in all experiments.

Copper electrodes(Alpha Metal 99.999%) were anodized in 14.7 mol l^{-1} phosphoric acid at 500 mA for 100 s. Zinc (Aldrich 99.999%) and lead(Merck 99.96%) electrodes were immersed in 10% w/w HNO_3 for 10 s and then washed many times with distilled water. Aluminum(Merck 99.95%) and carbon felt (Electrosynthesis Co.) were used without pretreatment. Palladium electrodes were prepared by electrodeposition using a $(CH_3COO)_2Pd$ (1% w/v) bath at a constant current density of 1 mA cm^{-2} for 1 h. The alloys were commercial screens (Alexandris Co.) of 100 mesh, Cu60Zn40 and Sn85Cu15, which were washed many times with $CHCl_3$ and water.

2.2. *Analytical methods*

At specific time intervals, samples of 0.1 ml were withdrawn from the catholyte by a chromatography syringe and after the appropriate dilution were analyzed. The determination of nitrate, nitrite and ammonia was performed by standard methods [33]. The determination of nitrate was based on its light absorption at 220 nm. Nitrite and ammonia were determined by the naphthyethylenediamine method (543 nm) and the phenate method (630 nm), respectively. Experiments for the possible formation of hydrazine and hydroxylamine were performed by colorimetric methods [34, 35].

A flowing stream of He (Figure 1) with a constant rate of 15 ml min^{-1} withdrew the gaseous products from the cell, when the analysis of the gaseous products was necessary. The solution was degassed for about 30 min before applying the voltage. The analysis of hydrogen, nitrogen and nitrous oxide was carried out by GC (molecular sieve 5A column 0.3175 cm i.d., 1.8 m) by using a temperature program from 80 (2 min) to 180 °C (65 °C min^{-1}) and a thermal conductivity detector (TCD). The detection limit of N_2O was relatively high and so only concentrations above 500 ppm could be measured. Nitric oxide and nitrogen dioxide were detected using an Environment S.A. (AC 30 M) analyzer.

The pH of the catholyte shifted towards more basic values during the electrolysis as a result of the electrochemical reactions that took place [36] and thus a part of the produced ammonia escaped from the cell due to the He stream. This amount was further stripped in a glass tube containing 0.5 M H_2SO_4 solution, which was connected following the cell as shown in Figure 1. In addition, another part of the produced ammonia passed through the Nafion membrane as ammonium cation and thus the analysis of the anolyte was necessary. Therefore, the total ammonia in the experimental results is the sum of the above-mentioned parts.

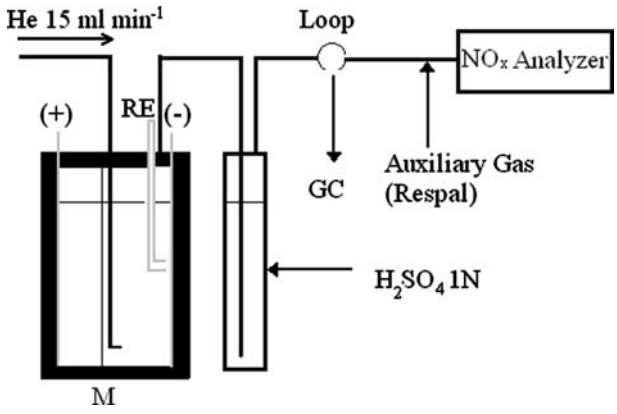

Fig. 1. Experimental set-up.

3. Results and discussion

3.1. *The influence of the electrode material*

Table 1 summarizes the experimental results of the reduction of NO_3^- on various metals and alloys. The % selectivity (%S) was calculated as the fraction of the produced moles of each product to the removed moles of nitrates multiplied by 100, apart from nitrogen, which was multiplied by two, since 2 mol of nitrate are needed for the formation of 1 mol of nitrogen. These results have a semi quantitative character, since the potential and the specific area of the electrodes were not the same. The selectivity of N_2 was high on Al(43%), Sn85Cu15 (35.3%) and Pb(17%). As far as we know aluminum has not been used for the electrochemical reduction of nitrate, but lead [19] and tin alloys, such as SnPt and SnPdAu [37–39] are known electrocatalysts for the conversion of nitrate to N_2. The increased %S of nitrogen on SnCu alloy, in comparison to that of copper, is possibly related to the higher overpotential of Sn for the hydrogen evolution reaction, which inhibits the hydrogenation of the produced nitrite to ammonia, leading the reaction to nitrogen.

The cyclic voltammograms of the reduction of nitrate on SnCu and Al, which are the most promising metals as regards the conversion of nitrate to nitrogen gas, are shown in Figure 2(a, b). The cathodic current due to hydrogen evolution on SnCu starts to increase at −1.65 V, while that of nitrate at −1.6 V. The irregular current fluctuations between −1.7 and −2.0 V in our system are likely to be caused by the formation of hydrogen bubbles at the electrode surface. The cyclic voltammogram on the Al (Figure 2b) cathode shows that the reduction of nitrate takes place at potentials more negative than −1.4 V and thus the overpotential on Al is lower by 0.2 V than that for bronze.

The main product on copper electrode is ammonia (Table 1) that is a hydrogenated product of the reduction. The selectivity for NH_3 formation was high (> 70%) on Cu, Cu60Zn40 and Zn, but the % removal efficiency (RE) of nitrate on Zn was significantly lower than the others. It should be mentioned that the selectivity of nitrogen oxides NO and NO_2 was very low in all cathodes and that hydroxylamine and hydrazine were not detected.

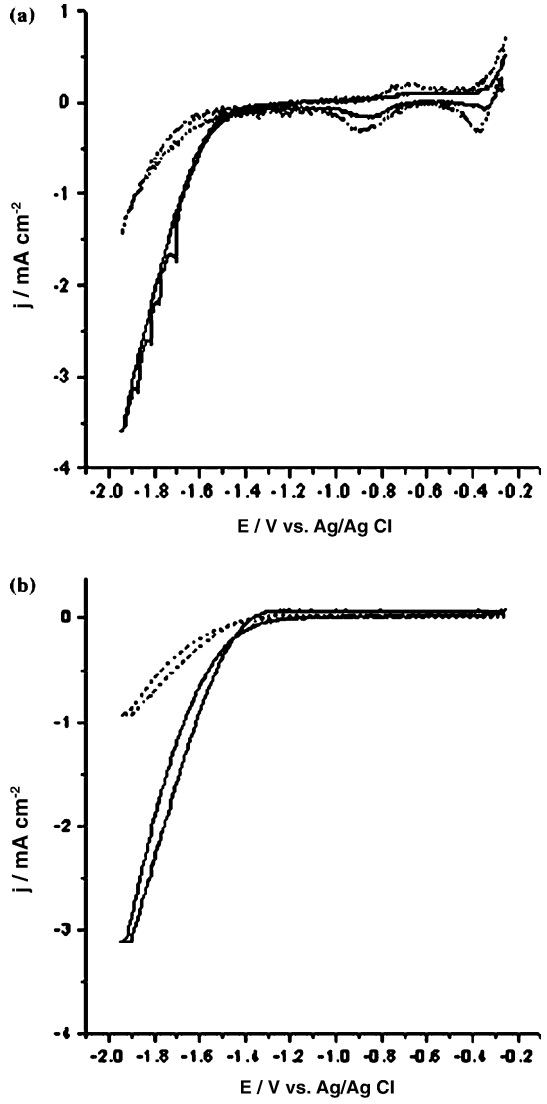

Fig. 2. (a,b) Cyclic voltammograms on (a) Sn85Cu15 and (b) Al without nitrate (—) and in 0.05 M KNO_3 (-). Scan rate is 20 mV s^1 and supporting electrolyte is 0.1 M K_2SO_4.

Table 1. Removal efficiency of nitrate and selectivity of the products at various electrodes and potentials. Electrolysis time 12 h

Cathode	E/V vs Ag/AgCl	NO_3^- % removal efficiency	% S				
			NO_2^-	NH_3	N_2	NO	NO_2
Cu	−1.5	90.0	11.1	77.3	1.0	[a]tr	0.1
Zn	−1.5	61.0	24.6	75.3	[b]nd	tr	tr
Al	−1.8	88.6	2.3	53.3	43.0	nd	nd
Pb	−2.0	93.3	0.1	68.5	17.1	0.1	0.02
Carbon felt	−2.0	94.9	15.2	73.8	3.5	tr	tr
Pd on carbon felt	−1.5	29.7	67.7	32.4	nd	tr	tr
Cu60Zn40	−1.5	99.1	9.6	75.2	2.1	0.8	0.1
Sn85Cu15	−1.6	55.0	85.8	3.6	13.9	nd	nd
Sn85Cu15	−2.0	97.4	17.4	41.1	35.3	0.01	0.5

[a]tr = traces.
[b]nd = not detected.

3.2. *Kinetic analysis of the experimental results on Sn85Cu15*

Even though Al was the most efficient cathode for the conversion of nitrate to N_2 the kinetic analysis was performed on Sn85Cu15, because the reproducibility of the experimental results was better. This is possibly due to the corrosion of the Al, during the experiment, from the produced hydroxide ions [36], through the formation of the $Al(OH)_4^-$ ion.

Figure 3 shows the concentration of nitrate, nitrite, ammonia and nitrogen at a constant potential of −2.0 V vs Ag/AgCl, as a function of electrolysis time, by considering nitrogen as a product of homogenous reaction. The concentration of nitrate follows a first-order exponential decay, while that of nitrite increases until 45 min and then decreases. A similar form of these curves has been previously reported by other workers on Pb [19] and Cu [25] and it is an indication that the reduction proceeds through a consecutive-reaction mechanism [40]. It should be noted that the reduction of nitrite under the same conditions gives nitrogen and ammonia. Based on the above the kinetic analysis was performed assuming the following reduction scheme:

$$NO_3^- \xrightarrow{k_1} NO_2^- \xrightarrow{k_2} NH_3$$

$$2NO_2^- \xrightarrow{k_3} N_2$$

The differential equations are:

$$\frac{d[NO_3^-]}{dt} = -k_1[NO_3^-] \quad (1)$$

$$\frac{d[NO_2^-]}{dt} = k_1[NO_3^-] - k_2[NO_2^-] - 2k_3[NO_2^-]^2 \quad (2)$$

$$\frac{d[NH_3]}{dt} = k_2[NO_2^-] \quad (3)$$

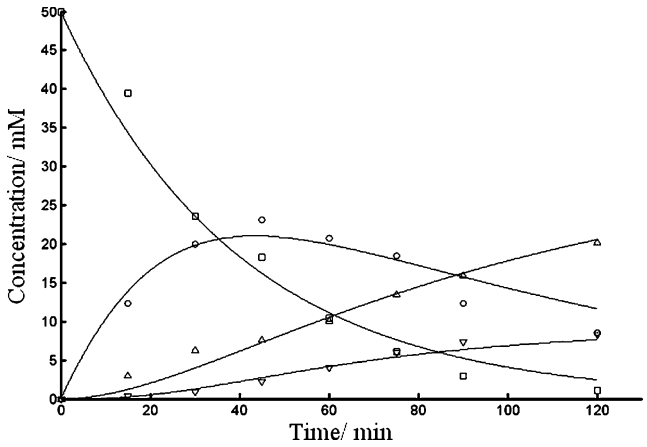

Fig. 3. Variation of the concentration of (□) nitrate, (○) nitrite, (△) ammonia and (▽) nitrogen against the electrolysis time on a Sn85Cu15 cathode at −2.0 V vs Ag/AgCl.

$$\frac{d[N_2]}{dt} = k_3[NO_2^-]^2 \quad (4)$$

The solution of the Equation (1) is:

$$[NO_3^-] = [NO_3^-]_o e^{-k_1 t} \Rightarrow \ln\frac{[NO_3^-]}{[NO_3^-]_o} = -k_1 t \quad (5)$$

where $[NO_3^-]_o$ is the initial concentration. The rate constant of the first step was found to be $k_1 = 4.9 \times 10^{-4}$ s^{-1} at −2.0 V, as the slope of the regression line of Equation (5).

The system of Equations (2–4) cannot be solved analytically and so the variable order Adams–Bashforth–Moulton predictor–corrector solver (PECE) method [41] (Mathlab 6.5) was used for the numerical solution and the estimation of the optimum values for the parameters k_2 and k_3. The initial conditions were $[NO_3^-]$ = 50 mM, $[NO_2^-]$ = 0, $[NH_3]$ = 0 and $[N_2]$ = 0. The calculated values were $k_2 = 1.76\times 10^{-5}$ s^{-1} and $k_3 = 7.66 \times 10^{-3}$ l mol^{-1} s^{-1}. In fact, the values of the rate constants include the hydrogen adsorption according to reference [42], where the rate of nitrate, when the hydrogen coverage is high, can be expressed as:

$$\frac{d[NO_3^-]}{dt} = -k(1-\vartheta_H)[NO_3^-]$$

When the hydrogen coverage ϑ_H is constant, the factor $k(1-\vartheta_H)$ can be replaced by a new constant k_1. This condition is satisfied in our case, because the experiments were performed in the region of hydrogen discharge, and thus the obtained values from the proposed model fit well to the experimental data, as shown in Figure 3, where the curves depict the theoretical predictions.

The total current is the sum of the partial currents of all the products and can be expressed as follows:

$$I = i_{NO_2^-} + i_{NH_3} + i_{N_2} + i_{H_2} \quad (6)$$

$$I = n_1 F\frac{d[NO_2^-]}{dt} + n_2 F\frac{d[NH_3]}{dt} + n_3 F\frac{d[N_2]}{dt} + n_4 F\frac{d[H_2]}{dt} \quad (7)$$

The number of electrons is: $n_1 = 2$, $n_2 = n_3 = 6$, $n_4 = 4$ and $F = 96{,}485$ C mol^{-1}.

Figure 4 shows the total current of the electrolysis and the calculated one from Equation (7). The partial currents of nitrite, ammonia and nitrogen were calculated after the differentiation of the corresponding curves of Figure 3 and the partial current of hydrogen was calculated after polynomial fitting of the experimental data. The simulation for the total current fits the experimental data, reasonably well if it is taken into account that it includes the total experimental error of the analysis. Furthermore, the simulation curve displays two local maxima for the current, which were observed experimentally, although the maxima were expected at shorter electrolysis times. The average current efficiencies (%CE) of the main

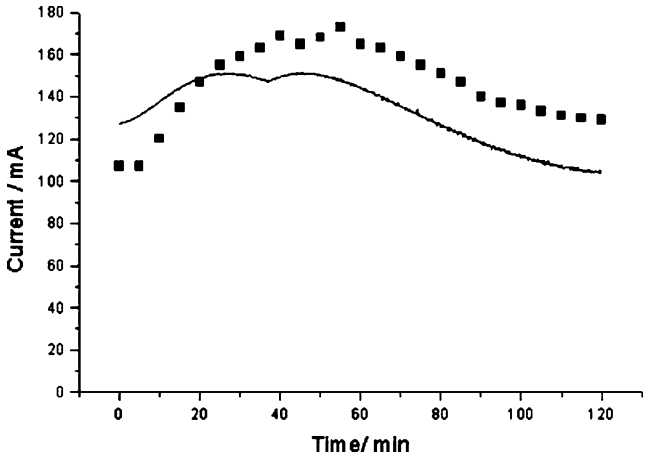

Fig. 4. Total current (■) and the simulated current vs electrolysis time at −2.0 V vs Ag/AgCl on a Sn85Cu15 cathode.

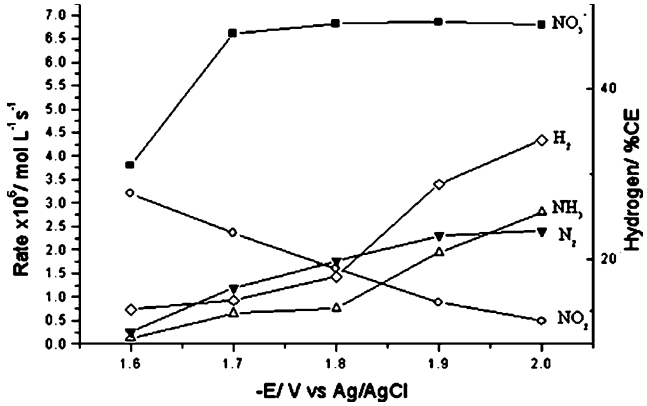

Fig. 5. Average rate of (■) nitrate, (○) nitrite, (△) ammonia, (▼) nitrogen and (◇) %CE of hydrogen as a function of the negative potential on Sn85Cu15. Electrolysis time 2 h.

products in this experiment were H_2: 28.2%, N_2: 15.1%, NO_2^-: 3.1% and NH_3: 47.9%.

3.3. *Effect of potential*

Figure 5 shows the average rate of formation of the main products on Sn85Cu15 at various potentials. The increase in potential favors the formation of N_2 and NH_3 and this is plausible if we assume that these products are formed through the reduction of the adsorbed NO, which is a potential controlled process as supported by other workers [26]. The increase in the rate of ammonia is more intense at potentials above −1.8 V, as a result of the increased hydrogen evolution in this potential region. This can be attributed to the fact that the formation of ammonia needs the hydrogenation of the adsorbed NO and therefore its rate is expected to increase with increase in the surface coverage by adsorbed hydrogen. The decrease in the rate of nitrite formation is typical for the intermediate product of the consecutive reactions mechanism [40].

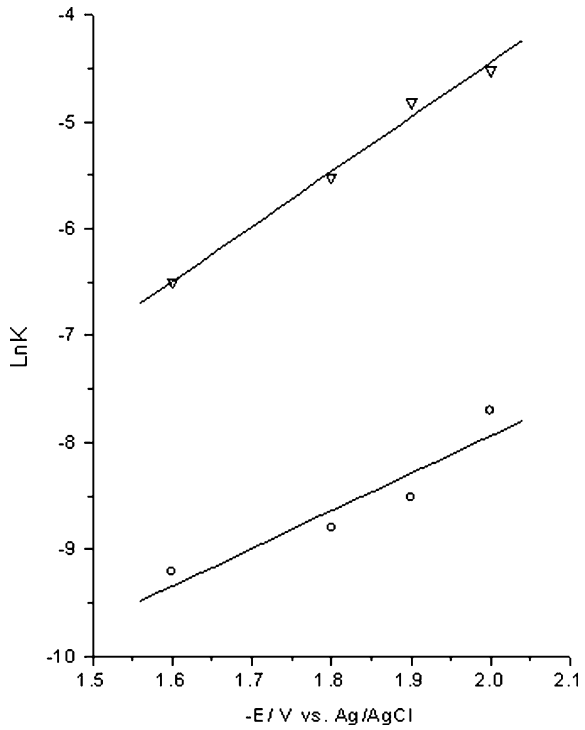

Fig. 6. Variation of the Lnk vs. the negative potential, (▽) k_2 and (○) k_3.

It should be noted that the rate of NO_3^- reduction is approximately the same in the potential regioin between −1.7 and −2.0 V. In order to clarify whether the reaction is limited by diffusion in this potential region, Fick's first law was applied assuming steady state conditions, linear axial concentration gradient, no radial diffusion and first order kinetics for the reduction of nitrate. The initial flux of nitrate is [43]:

$$N = \frac{DC_o}{b}\sqrt{\frac{k_1 b^2}{D}}\tanh\sqrt{\frac{k_1 b^2}{D}} \tag{8}$$

where N = flux rate(mol m^{-2} s^{-1}), D = diffusion coefficient of the nitrate in water (1.9×10^{-9} m^2 s^{-1}) [44], C_0 = the initial concentration of the nitrate (50 mol m^{-3}), b = the length of the cathode space(0.015 m) and $k_1 = 4.9 \times 10^{-4}$ s^{-1}. By substituting these values in equation (8) we obtain $N = 4.8 \times 10^{-5}$ mol m^{-2} s^{-1}. The apparent area of the cathode was $A = 13.3 \times 10^{-4}$ m^2 and thus the total diffusion rate is $r_d = N{\cdot}A = 6 \times 10^{-8}$ mol s^{-1}. The initial rate of reduction of nitrate from the experimental data was found to be 3.1×10^{-7} mol s^{-1} at −2.0 V. The fact that the measured rate is higher than the predicted one from equation (8) can be attributed to the participation of forced convection, due to the He stream and to the roughness factor of the electrode, which was not taken into account.

The effect of the potential is given by Equations (1–4) by replacing the potential dependence of the rate constant k_i (i = 1, 2, 3) by:

$$k_i = k_i^0 e^{-a_i\vartheta} \Rightarrow \ln k_i = k_i^0 - a_i\vartheta \tag{9}$$

Table 2. Removal efficiency of nitrate and selectivity of the products at various electrodes and potentials in a divided and in an undivided cell. Electrolysis time 12 h

Electrode material	E/V vs Ag/AgCl	Divided cell				Undivided cell			
		%RE		%S		%RE		%S	
		NO_3^-	NO_2^-	NH_3	Gases	NO_3^-	NO_2^-	NH_3	Gases
Cu60Zn40	−1.50	99.1	9.6	75.2	3.0	91.5	3.1	34.6	62.3
Sn85Cu15	−2.00	97.4	17.4	41.1	35.3	93.4	1.9	18.5	79.6
Sn85Cu15	−1.90	98.8	22.6	28.5	34.6	92.1	4.7	12.8	82.5
Al	−1.80	88.6	2.3	53.3	43.0	82.1	0.6	35.3	64.1
Pb	−2.00	93.3	0.1	68.5	17.2	86.4	1.1	45.3	53.6

where k_i^0 is the rate constant at zero potential, a_i the charge transfer coefficient, $\vartheta = EF/RT$ and E is the potential vs NHE.

Equation (9) shows that the logarithm of the rate constant is in a linear relationship with the potential. The values of k_1, k_2 and k_3 at each potential can be calculated as mentioned above by the numerical method. The plot of lnk as a function of potential gives the k_i^0 as intercept and the charge transfer coefficient (a_i) as the slope. Figure 6 shows that the experimental results follow the above-mentioned relationship, since the correlation coefficients for the $\ln k_2$ and $\ln k_3$ were found to be 0.994 and 0.945, respectively. The logarithm of k_1 is not depicted in Figure 6 because the reduction of nitrate to nitrite in this potential region is a diffusion-limited process. The slope for $\ln k_2$ vs E was found to be 5.12 and thus $\alpha_2 = 0.131$. In the same way we obtain $\alpha_3 = 0.089$.

3.4. *Electrolysis in an undivided cell*

The experimental results clearly show that Sn85Cu15 is an efficient electrocatalyst for the reduction of nitrate, since both the reduction rate and the selectivity of N_2 are high. In order to oxidize the produced ammonia and nitrite on the anode of the cell some experiments were conducted in an undivided cell.

Table 2 shows the % removal efficiency of nitrate and the selectivity of nitrite and ammonia in a divided and an undivided cell on various electrodes. The selectivity of the gases in the undivided cell was obtained by abstraction of the selectivities of nitrite and ammonia from 100%. The comparison between the two cell configurations shows that the concentration of the byproducts is lower in the undivided cell in all the examined cases. For example, on Sn85Cu15 at −1.9 V the %S of ammonia and nitrite are by 2.2 and 4.8 times lower respectively. When the electrolysis was continued for 24 h the %S of the products were not significantly different, because of the low rate of diffusion of ammonia and nitrite to the anode. In contrast, the removal efficiency of nitrate is lower in the undivided cell. In order to confirm if the decrease in the %RE of nitrate was due to the partial oxidation of the produced ammonia to the initial nitrate on the anode, we performed two experiments on the anodic oxidation of ammonia from a solution containing 0.1 M K_2SO_4 and 0.05 M $(NH_4)SO_4$ on Pt anode at 2.3 and 2.5 V vs Ag/AgCl. These potentials were selected because the observed anodic potential in the undivided cell was in this range. The experimental results showed that the %RE of ammonia was 12 and 15% and the %S of nitrate was 85 and 92%, respectively. This result is in agreement with a previous study by Gootzen et al. [45], who pointed out that when the surface of the anode becomes oxidized, the oxidation of ammonia leads exclusively to oxygen containing compounds.

In conclusion, our experimental results indicated that even though the final concentration of ammonia and nitrite is lower in the undivided cell it is difficult to achieve environmentally acceptable values in this way. This work is in progress by applying rapid square wave potential pulses with the appropriate anodic and cathodic limits and frequency [46].

References

1. O. Strebel, W.H.M. Duynisveld and J. Boettcher, *Agric. Ecosyst. Environ.* **26** (1989) 189.
2. EEC Council directive on the quality of water for human consumption (No-80/778 off), *J. EEC.* **229** (1980) 11–29.
3. WHO, *Guidelines for Drinking water Quality*, Geneva 1993.
4. V. Mateju, S. Cizinska, J. Krejci and J. Tomas, *Enzyme. Microb. Tech.* **14** (1992) 170.
5. L. Panyor and C. Fabiani, *Desalination* **104** (1996) 165.
6. J.J. Schoeman and A. Steyn, *Desalination* **155** (2003) 15.
7. K.N. Mani, *J. Membrane Sci.* **58** (1991) 117.
8. C. Huang, H. Warg and P. Chiu, *Wat. Res.* **32** (1998) 2257.
9. W. Gao, N. Guan, J. Chen, G. Gyan, R. Jin, H. Zeng, Z. Liu and F. Zhang, *Appl. Catal. B* **46** (2003) 341.
10. F. Gauthard, F. Epron and J. Barbier, *J. Catal.* **220** (2003) 182.
11. C. Ottley, N. Davison and W. Edmunds, *Geochim. Cosmochim. Acta* **61** (1997) 1819.
12. K. Inazu, M. Kitahara and K. Aika, *Catal. Today* **93–95** (2004) 263.
13. U. Prusse, M. Hahnlein, J. Daum and K.D. Vorlop, *Catal. Today* **55** (2000) 79.
14. W. Gao, N. Guan, J. Chen, X. Guan, R. Jin, H. Zeng, Z. Liu and F. Zhang, *Appl. Catal. B* **46** (2003) 341.
15. M. Paidar, I. Rousar and K. Bouzek, *J. Appl. Electrochem.* **29** (1999) 611.
16. S. Ureta and C. Yanez, *Electrochim. Acta* **42** (1997) 1725.

17. J. Gootzen, P. Peeters, J. Dukers, L. Lefferts, W. Visscher J. Van Veen, *J. Electroanal. Chem.* **434** (1997) 171.
18. H. Li, D. Robertson, J. Chambers and D. Hobbs, *J. Electrochem. Soc.* **135** (1988) 1154.
19. J. Bockris and J. Kim, *J. Appl. Electrochem.* **27** (1997) 623.
20. L.J.J. Janssen, M.M.J. Pieterse and E. Barendrecht, *Electrochim. Acta* **22** (1976) 27.
21. O. Rutten, A. Van Sandwijk and G. Van Weert, *J. Appl. Electrochem.* **29** (1999) 87.
22. Y. Xiang, D. Zhou and J.F. Rushling, *J. Electroanal. Chem.* **424** (1997) 1.
23. N. Chebotareva and T. Nyokong, *J. Appl. Electrochem.* **27** (1997) 975.
24. J.O'M. Bockris and J. Kim, *J. Electrochem. Soc.* **143** (1996) 3801.
25. K. Bouzek, M. Paidar, A. Sadlikova and H. Bergmann, *J. Appl. Electrochem.* **31** (2001) 1185.
26. A.C.A. Vooysde, R.A. Santenvan and J.A.R. van Veen, *J. Mol. Catal. A* **154** (2000) 203.
27. G. Horanyi and E.M. Rizmayer, *J. Electroanal. Chem.* **143** (1983) 323.
28. G. Horanyi and E.M. Rizmayer, *J. Electroanal. Chem.* **331** (1992) 897.
29. H.L. Li, J.Q. Chambers and D.T. Hobbs, *J. Appl. Electrochem.* **18** (1988) 454.
30. G.E. Dima, A.C.A. Vooysde and M.T.M. Koper, *J. Electroanal. Chem.* **554** (2003) 15.
31. J.F.E. Gootzen, L. Lefferts and J.A.R. Van Veen, *Appl. Catal.* **188** (1999) 127.
32. J. Genders, D. Hartsough and D. Hobbes, *J. Appl. Electrochem.* **26** (1996) 1.
33. L.S. Clesceri, A.E. Greenberg, R.R. Trussell, 'Standard Methods for the Examination of Water and Wastwater', 17th edn. (American Public Health Association, Washington, DC, 1989), pp. 4–120, 4–129 and 4–131.
34. G.W. Watt and J.D. Chrisp, *Anal. Chem.* **24** (1952) 2006.
35. F. Dias, A.S. Olojola and B. Jaselskis, *Talanta* **26** (1979) 47.
36. S. Kerkeni, E. Lamy-Pitara and J. Barbier, *Catal. Today* **75** (2002) 35.
37. K. Shimazu, R. Goto and K. Tada, *Chem. Lett.* **2** (2002) 204.
38. K. Tada, T. Kawaguchi and K. Shimazu, *J. Electroanal. Chem.* **572** (2004) 93.
39. K. Shimazu, T. Kawaguchi and K. Tada, *J. Electroanal. Chem.* **529** (2002) 20.
40. G. Sakellaropoulos, *AIChE J.* **25** (1979) 781.
41. J.C. Butcher, *J. Comp. Appl. Math.* **125** (2000) 1.
42. D. De, E.E. Kalu, P.P. Tarjan and J.D. Englehardt, *Chem. Eng. Technol.* **27** (2004) 56.
43. R.B. Bird, W.E. Stewart and E.N. Lightfoot, 'Transport Phenomena' (J. Wiley & Sons, 1960) 533 pp..
44. R.C. Reid, J.M. Prausnitz and B.E. Poling, *The Properties of Gases and Liquids*, 4th ed., (McGraw Hill Inc., New York, 1987).
45. J.F.E. Gootzen, A.H. Wonders, W. Visscher, R.A. Santenvan and J.A.R. Veenvan, *Electrochim. Acta* **43** (1998) 1851.
46. C. Polatides, M. Dortsiou and G. Kyriacou, Proceedings of 55th ISE Meeting Thessaloniki, September 2004, 333pp.
47. H. Li, D.H. Robertson, J. Chambers and D. Hobbs, *J. Electrochem. Soc.* **135** (1988) 1154.